

Decoupling of superconducting V by ultrathin Fe layers in V/Fe multilayers

P. Koorevaar

Kamerlingh Onnes Laboratorium der Rijksuniversiteit Leiden, P.O. Box 9506, 2300 RA Leiden, The Netherlands

Y. Suzuki

*Philips Research, P.O. Box 80 000, 5600 JA Eindhoven, The Netherlands
and Hitachi Central Research Laboratory, P.O. Box 2, Kokubunji, Tokyo 185, Japan*

R. Coehoorn

Philips Research, P.O. Box 80 000, 5600 JA Eindhoven, The Netherlands

J. Aarts

Kamerlingh Onnes Laboratorium der Rijksuniversiteit Leiden, P.O. Box 9506, 2300 RA Leiden, The Netherlands

(Received 27 April 1993)

We report on a detailed study of superconducting critical temperatures T_c and critical fields H_{c2} of V/Fe multilayers. The thickness of the V layers (d_V) and Fe layers (d_{Fe}) as well as the total number of layers in the multilayer (N) were varied systematically. For $d_{Fe} \geq 0.6$ nm, at constant d_V , T_c and the critical fields for parallel ($H_{c2\parallel}$) and perpendicular ($H_{c2\perp}$) orientation do not depend on either d_{Fe} or N , and a two-dimensional (2D) temperature dependence for $H_{c2\parallel}$ without 3D-2D crossover is observed for small values of d_V . The predicted oscillatory behavior of T_c as a function of d_{Fe} is not found. We conclude that the superconducting V layers are completely decoupled by only 0.6 nm Fe, in conflict with previous reports. Upon decreasing d_V at constant d_{Fe} , a strong decrease of T_c is found. This, together with the temperature dependence of $H_{c2\parallel}$ and $H_{c2\perp}$ for all samples can be described by existing theory.

I. INTRODUCTION

Because of the strong pair-breaking effect in ferromagnetic (F) layers, the superconducting (S) properties of a S/F multilayer can be strongly influenced even by very thin F layers. This was already known from experiments by Hauser, Theuerer, and Werthamer¹ on bilayers with $S=\text{Pb}$ and $F=\text{Fe, Ni, or Gd}$, and shown once more by Wong *et al.*^{2,3} on the V/Fe system. The latter experiments show that the critical temperature T_c of S/F multilayers and $F/S/F$ sandwiches drastically decreases with decreasing S -layer thickness d_S , even if the F layer consists of a few atomic planes. The predominant pair-breaking mechanism in the F layers is thought to be the polarization of the conduction electrons by the strong exchange field, and for not too thin Fe layers this will decouple the superconducting layers. Not quite clear, however, is whether coupling becomes possible when the F layer is very thin (although ordered) and tunneling becomes possible. From the occurrence of a three-dimensional (3D) to two-dimensional (2D) crossover in $H_{c2\parallel}(T)$, Wong *et al.* concluded that this is indeed the case in V/Fe layers for Fe-layer thicknesses less than 1.3 nm (six atomic planes in their units).³ The possibility for this is the more interesting since such a coupling might be due to an exotic mechanism, which was recently investigated by Radović *et al.*^{4,5} and by Buzdin, Kupriyanov, and Vujčić.⁶ The order parameter would behave similar to the order parameter in a “ π -contact” superconducting interferometer,⁷ in which the phase difference between two neighboring S layers would no longer be 0, but could

take a value between 0 and π . For an S/F multilayer, the consequence is that T_c oscillates as function of the thickness of the F layer, d_F . An experimental indication for such behavior was found in V/Fe multilayers,³ but the data points are scarce and the existence of the π phase has not been shown unambiguously.

Theoretical calculations also exist for the case of decoupled S layers.⁴ A second motivation for the underlying investigation of V/Fe multilayers therefore was to make a systematic comparison between these calculations and the experiments.

Below, we describe two types of experiments. In the first we tried to observe T_c oscillations in V/Fe multilayers by varying the Fe-layer thickness from 0.2 to 6.0 nm. The V-layer thicknesses are chosen in the range for which the T_c oscillations are indicated by both the experimental results of Wong *et al.*³ and the theoretical calculations in Ref. 5. As we will show below, the multilayers have excellent compositional, magnetic, and superconducting characteristics. However, in these high-quality samples T_c oscillations as function of d_{Fe} were not observed, in conflict with results reported in Ref. 3. On the contrary, our results indicate that only 0.6-nm-thick Fe layers completely decouple the V layers. For $d_{Fe} \geq 0.6$ nm, both T_c , $H_{c2\parallel}$, and $H_{c2\perp}$ do not depend on d_{Fe} or on the total number of layers in the multilayer, as expected if the V layers are completely decoupled. Also, if the individual V layers are thin enough, $H_{c2\parallel}(T)$ shows the well-known two-dimensional behavior $H_{c2\parallel} \propto \sqrt{1-T/T_c}$ in a wide temperature range. This has to arise from single V films, since the total sample thickness would not allow 2D

behavior. In the second type of experiments, we investigated the behavior of T_c and $H_{c2}(T)$ as function of V-layer thickness of multilayers with decoupled V layers. As expected, T_c decreases drastically with decreasing d_V , in accordance with previously reported results.^{1,3} This is again an indication that our multilayers are of good quality. The data for T_c vs d_V and both the $H_{c2\perp}$ and $H_{c2\parallel}$ vs T curves for different d_V can all be fitted to the theory mentioned above,⁴ where only one free adjustable parameter is needed.

II. EXPERIMENTAL DETAILS

Most series of multilayers were grown by dc magnetron sputtering (base pressure 5×10^{-7} mbar). One series was grown by molecular-beam epitaxy (MBE) (base pressure 5×10^{-10} mbar). In all cases the substrates were Si(001). The oxide layer was removed *ex situ* by dipping into a HF solution, and before deposition the surface was cleaned by glow discharge. During deposition, the substrates were kept at room temperature, while typical growth rates were 0.2 nm/s. X-ray diffraction was performed on one sputtered series and on the MBE-grown series. The high-angle data indicate that both V and Fe have bcc structure, but that the texture of the films is different for the two growth methods. The MBE-grown samples predominantly have (100) texture, while the sputtered samples showed (110) texture. The atomic plane distance is therefore 0.3 nm (V) and 0.29 nm (Fe) in the MBE case, but 0.21 nm (V) and 0.20 nm (Fe) for the sputtered samples. As we will see below, this apparently does not influence the superconducting or magnetic properties. At low angles, clear superlattice peaks were observed from which a period could be determined as a check on the growth rates.

Five different sets of multilayers were made with varying inner layer thicknesses and both V and Fe outer layers. We use the following notation: 44 nm V/3(0.6 nm Fe/44 nm V) means a sample with 44 nm V as the bottom layer, followed by three blocks of 0.6 nm Fe/44 nm V. The top and bottom layers were always from the same material and equally thick (i.e., the multilayers were all completely symmetrical). Two sets had V outer layers and varying Fe-layer thicknesses. One of these was MBE grown with thicknesses 40 nm V/3(d_{Fe} Fe/40 nm V), and one was sputtered with thicknesses 44 nm V/3(d_{Fe} Fe/44 nm V), having $d_{Fe} = 0.6, 1.0, 1.6, 2.4,$ and 6.1 nm, as well as $d_{Fe} = 3.2$ nm in the MBE-grown set.

Two sets had Fe outer layers, in which the inner Fe-layer thickness was varied [3 nm Fe/2(40 nm V/ d_{Fe} Fe)/(3 nm $-d_{Fe}$)Fe with $d_{Fe} = 0.1, 0.2, 0.4, 0.6, 0.8,$ and 1.6 nm] or the number of blocks [3 nm Fe/ N (40 nm V/1.0 nm Fe)/2 nm Fe, with $N = 2, 3, 4,$ and 5]. In the final set, the V thickness was varied with constant Fe thickness, 5 nm Fe/2(d_V V/3.0 nm Fe)/2 nm Fe, with d_V between 10 and 100 nm. In all cases the sample dimensions were 12×4 mm². The sets where the Fe-layer thickness was varied were used to investigate the decoupling of the V layers by the Fe layers. In the set with varying V-layer thickness, the V layers are decoupled. The superconducting properties of these multilayers strongly depend upon

d_V , a result which can serve as a test for the model put forward in Ref. 5. For comparison, a MBE-grown V monolayer and a sputtered V monolayer of 150 nm thickness have also been measured.

In order to gain insight into the magnetic properties of our multilayers, we took magnetization curves at room temperature with a vibrating-sample magnetometer on all samples with V outer layers, i.e., MBE-grown 40 nm V/3(d_{de} Fe/40 nm V) and sputtered 44 nm V/3(d_{Fe} Fe/44 nm V), with d_{Fe} variable. The field was applied parallel to the layers. Note that in order to extract the magnetic behavior of the thin inner Fe layers, it is necessary that the multilayers do not have protective Fe top and bottom layers. A typical magnetization curve for the sputtered sample 44 nm V/3(1.0 nm Fe/44 nm V) is shown in Fig. 1(a). Saturation of the magnetization was reached in fields below 0.13 T for all multilayers. The decrease of the magnetic signal for fields above the saturation field is due to the background, and it is only observable for multilayers having thin Fe layers. Figure 1(b) shows the saturation magnetization vs Fe-layer thickness for both sets of multilayers. The drawn straight line in the figure shows the magnetization assuming a bulk moment on the Fe atoms ($2.2\mu_B$ corresponding to an internal field of 2.15 T) and no magnetic signal from the V layers. The data fall on a straight line with the same slope as for the bulk magnetization, as indicated by the dotted

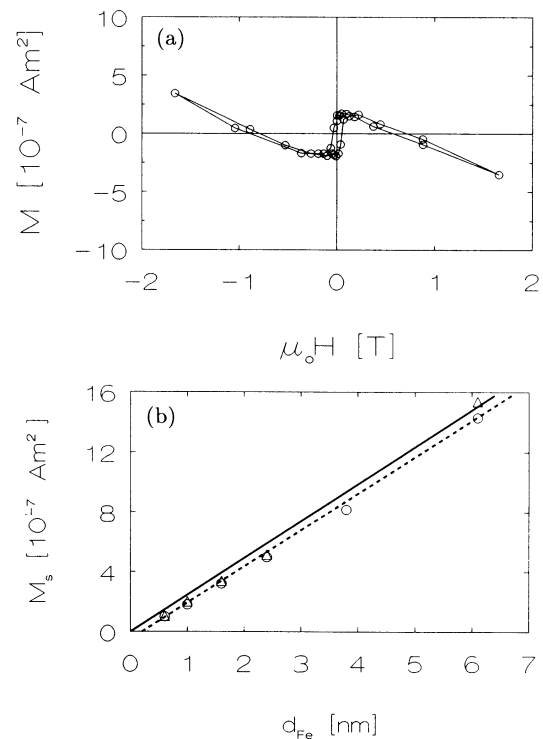


FIG. 1. (a) Magnetization vs applied field for the sputtered sample 44 nm V/3(1.0 nm Fe/44 nm V). (b) Saturation magnetization for samples 44 nm V/3(d_{Fe} Fe/44 nm V) (sputtered) (Δ) and 40 nm V/3(d_{Fe} Fe/40 nm V) (MBE grown) (\circ). The solid line is expected for an Fe atom bulk moment of $2.2\mu_B$. The dotted line is a guide to the eye, indicating 0.1 nm magnetically dead Fe material on the interfaces.

line. However, the x axis is intercepted at 2 \AA . Since the effective moment on Fe atoms decreases drastically with increasing V concentration in V/Fe alloys,⁸ this result indicates that either a dead layer exists of about 1 \AA when the interface is perfectly sharp or mixing occurs over no more than one atomic plane. From these results we infer that the Fe atoms have a well-defined moment, even in very thin Fe layers.

The superconducting properties T_c , $H_{c2\parallel}(T)$, and $H_{c2\perp}(T)$ were measured resistively in a standard four-terminal configuration and defined at the midpoint of the superconducting-normal transition. H_{c2} was measured by sweeping the field at constant temperature. The samples showed good superconducting properties, with ΔT_c as defined by a 10–90% transition width typically less than 20 mK and very sharp transitions in the field.

III. RESULTS AND DISCUSSION

A. Decoupling by ultrathin Fe layers

In Fig. 2, T_c 's are shown for all sets of multilayers where the Fe-layer thickness was varied, together with the results for the 150-nm-thick V monolayers and one sample from another set with the same V thickness [5 nm Fe/2(40 nm V/3.0 nm Fe)/2 nm Fe]. The well-known effect of T_c reduction by even very thin Fe layers is reproduced. For $d_{\text{Fe}} \geq 0.6 \text{ nm}$, T_c is independent of d_{Fe} , indicating that Fe layers with $d_{\text{Fe}} = 0.6 \text{ nm}$ already completely decouple the V layers.

For $d_{\text{Fe}} \leq 0.4 \text{ nm}$, T_c is strongly influenced by d_{Fe} . This may be caused both by a decrease of the moment on the Fe atoms in these very thin Fe layers and by the fact that the V layers are not completely decoupled anymore. Note that a hypothetical multilayer in the set 3 nm Fe/2(40 nm V/ d_{Fe} Fe)/(3 nm – d_{Fe}) Fe with $d_{\text{Fe}} = 0 \text{ nm}$ should not be compared to the 150-nm-thick monolayers,

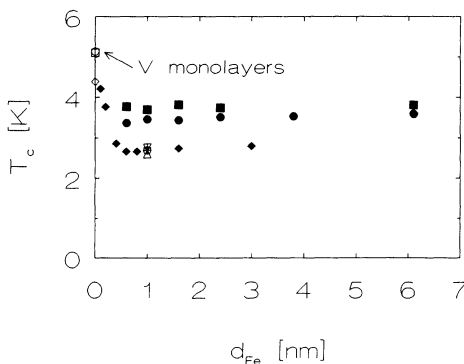


FIG. 2. T_c vs d_{Fe} for different multilayers; with V outer layers: 44 nm V/3(d_{Fe} Fe/44 nm V) (■) and 40 nm V/3(d_{Fe} Fe/40 nm V) (MBE grown) (●); with Fe outer layers: 3 nm Fe/2(40 nm V/ d_{Fe} Fe)/(3 nm – d_{Fe}) Fe (◆), supplemented with 5 nm Fe/2(40 nm V/3.0 nm Fe)/2 nm Fe; with varying number of blocks: 3 nm Fe/ N (40 nm V/1.0 nm Fe)/2 nm Fe with $N=2$ (▽), $N=3$ (⊕), $N=4$ (+), $N=5$ (△). Also shown are monolayers of 150 nm, sputtered (□) and MBE grown (○), and multilayer 5 nm Fe/2(85 nm V/3.0 nm Fe)/2 nm Fe (◇).

but rather to one 80-nm-thick V layer sandwiched between two Fe layers, which already has a lower T_c than bulk V. Therefore T_c for sample 5 nm Fe/2(85 nm V/3.0 nm Fe)/2 nm Fe is also shown. The difference in T_c for the sputtered multilayers from the sets 44 nm V/3(d_{Fe} Fe/44 nm V) and 3 nm Fe/2(40 nm V/ d_{Fe} Fe)/(3 nm – d_{Fe}) Fe is mainly caused by the difference in top and bottom layers. When the outer layers consist of Fe, all V layers are identical. Outer layers of V, however, will not be identical to inside V layers, since they have Fe on one side only. The depression of the order parameter due to the S/F interface, which will be discussed in more detail later, will therefore be less in the outer layers, leading to a higher T_c . If the Fe layers decouple the V layers, this is the T_c measured and shown in Fig. 2.

Concentrating on the multilayers in the set 3 nm Fe/ N (40 nm V/1.0 nm Fe)/2 nm Fe, we see that varying the number of layers in a multilayer does not influence T_c , even though the inner Fe layers are only 1 nm thick. This is as expected when only 0.6 nm of Fe decouples the V layers completely. These results are also interesting with respect to theoretical calculations by Kulik,⁹ which indicate that the T_c of a multilayer can depend on the number of layers if a weak electron correlation between the S layers is present. This electron correlation is different from electron transfer by Josephson coupling or a proximity effect. Experimentally, T_c dependence on number of layers was observed in Ag-In and Ag-Sn multilayers.¹⁰ If the approximations in Ref. 9 are appropriate, our result that the number of layers does not influence T_c is further evidence that the V layers are completely decoupled.

To check this main finding, we also measured the critical fields. In Fig. 3 we show $H_{c2\parallel}$ vs T for several samples with inner Fe layers of 0.6 nm and, for comparison, for some samples with thicker Fe layers. Concentrating on the multilayers with $d_{\text{Fe}} = 0.6 \text{ nm}$, we observe that $H_{c2\parallel}$ for all three samples behaves in agreement with the ex-

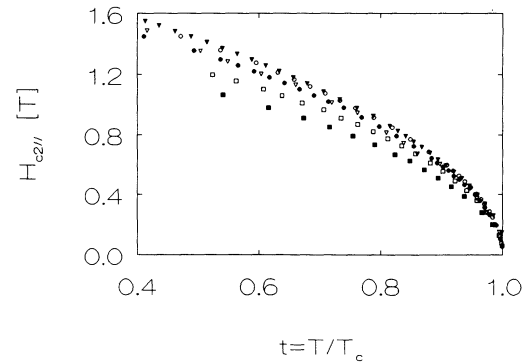


FIG. 3. $H_{c2\parallel}$ for multilayers with different outer layers and different d_{Fe} : 44 nm V/3(0.6 nm Fe/44 nm V) (▼) and 44 nm V/3(2.4 nm Fe/44 nm V) (▽); 40 nm V/3(0.6 nm Fe/40 nm V) (MBE grown) (●) and 40 nm V/3(2.4 nm Fe/40 nm V) (MBE grown) (○); 3 nm Fe/2(40 nm V/0.6 nm Fe)/2.4 nm Fe (■) and 3 nm Fe/2(40 nm V/1.6 nm Fe)/1.4 nm Fe (□). All solid symbols represent samples with inner Fe layers of 0.6 nm.

pectation for a two-dimensional thin film in a parallel field,

$$H_{c2\parallel}(T) = H_{c2\parallel}(0)(1 - T/T_c)^{1/2}. \quad (1)$$

This is especially clear from the inset in Fig. 4, where $H_{c2}(T)/(1 - T/T_c)^{1/2}$ is plotted. This 2D behavior is observed up to $T/T_c = 1$; i.e., a transition from 2D to 3D behavior is not observed. This is again a strong indication that V layers are decoupled, since the total sample thicknesses are too large for 2D behavior to occur over more than a fraction of the temperature range if V layers were not decoupled. It should be mentioned that in Ref. 3 clear 3D to 2D transitions were observed in V/Fe multilayers with Fe layers of 0.6 nm, indicating that in those samples the Fe layers did not decouple the V layers completely. Comparing each of the three samples with a sample from the same set but with thicker Fe-layer thickness, we see (inset of Fig. 4) that values for $H_{c2\parallel}(0)$ for samples within the same set differ less than 12%, with no systematics regarding Fe-layer thickness. $H_{c2\parallel}(0)$ does depend upon the material of top and bottom layers, being larger for samples with V on top and bottom. In the same way as discussed for T_c , this means that $H_{c2\parallel}$ is larger for the outer V layers. It is interesting to note that $H_{c2\parallel}(T)$ of these outer layers still shows the square-root behavior expected for thin films. Single V films of 40 nm would show 3D behavior at low temperature, since this thickness is larger than twice the zero-temperature coherence length of 13.9 nm (see below).

In Ginzburg-Landau (GL) theory for a single thin film in vacuum, $H_{c2\parallel}(0)$ as defined in Eq. (1) can be written as $H_{c2\parallel}(0) = \phi_0 \sqrt{12/2\pi\xi(0)d}$, with ϕ_0 the flux quantum, $\xi(0)$ the zero-temperature GL coherence length, and d the thickness of the film. In the next section, we will show that, as a result of the different boundary conditions, this factor is different for $F/S/F$ sandwiches or S/F bilayers. It depends upon the F material and does not have a sim-

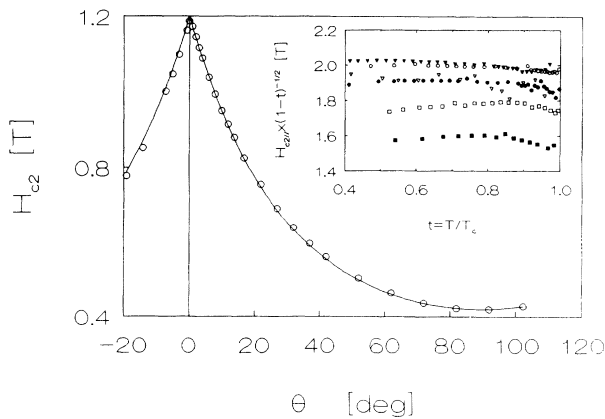


FIG. 4. Angular dependence of the critical field for sample 44 nm V/3(0.6 nm Fe/44 nm V) at $T = 2.5$ K ($t = 0.66$). The line is a fit to the 2D expression [Eq. (2)]. The inset shows $H_{c2\parallel}(t)$ divided by $(1 - t)^{1/2}$ vs t for the data of Fig. 3. Symbols are the same as in Fig. 3.

ple functional form with respect to d_S . Nevertheless, the angular dependence of $H_{c2}(\theta)$, with θ the angle between the layers and the field, is still correctly described by the Tinkham expression for a thin film in vacuum,

$$\left| \frac{H_{c2}(\theta)\sin(\theta)}{H_{c2\perp}} \right| + \left| \frac{H_{c2}(\theta)\cos(\theta)}{H_{c2\parallel}} \right|^2 = 1. \quad (2)$$

This is seen from Fig. 4, where $H_{c2}(\theta)$ is plotted for one sample with 0.6-nm-thick Fe layers, measured at $T = 2.5$ K ($t = 0.66$). The line is a fit to Eq. (2), and the agreement is remarkably good.

Not only $H_{c2\parallel}$ but also $H_{c2\perp}$ for the multilayers should be independent of d_{Fe} if V layers are decoupled. In Fig. 5, $H_{c2\perp}$ is plotted versus reduced temperature for the sputtered samples for which $H_{c2\parallel}$ was shown in Fig. 3. Also shown is the result for a sputtered V monolayer with thickness 150 nm. All measurements show a linear T dependence near T_c . It is indeed observed that the Fe-layer thickness does not influence the H_{c2} curves. The difference in $H_{c2\perp}$ at any T is less than 8% for multilayers from the same set.

The temperature dependence of $H_{c2\perp}$ near T_c is, in GL theory, given by

$$H_{c2\perp}(T) = \frac{\phi_0}{2\pi\xi(0)^2}(1 - T/T_c). \quad (3)$$

Then, for the slope S of $H_{c2\perp}$ with the reduced temperature $t = T/T_c$, one has

$$S = - \left. \frac{\partial H_{c2\perp}}{\partial t} \right|_{t=1} = \frac{\phi_0}{2\pi\xi(0)^2}. \quad (4)$$

The values for S in Fig. 5 are clearly not all the same, even though the V layers have the same $\xi(0)$. Again, this is mainly due to the different material of top and bottom layers. For the multilayer with V as outside layers, the behavior of H_{c2} is again completely determined by only the outside layers. The value for S for these multilayers is apparently larger than for multilayers with Fe as out-

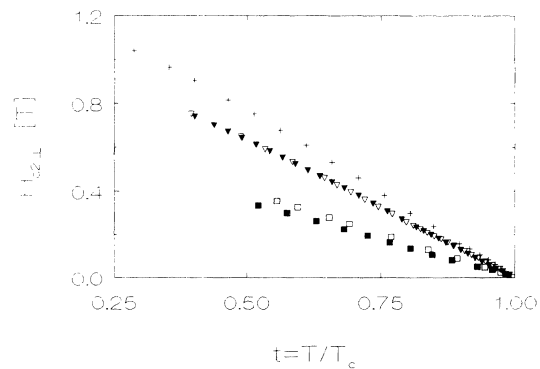


FIG. 5. $H_{c2\perp}$ for multilayers with different outer layers and different d_{Fe} : 3 nm Fe/2(40 nm V/0.6 nm Fe)/2.4 nm Fe (\blacksquare) and 3 nm Fe/2(40 nm V/1.6 nm Fe)/1.4 nm Fe (\square); 44 nm V/3(0.6 nm Fe/44 nm V) (\blacktriangledown) and 44 nm V/3(2.4 nm Fe/44 nm V) (\triangledown); also shown is the 150-nm-thick sputtered monolayer ($+$).

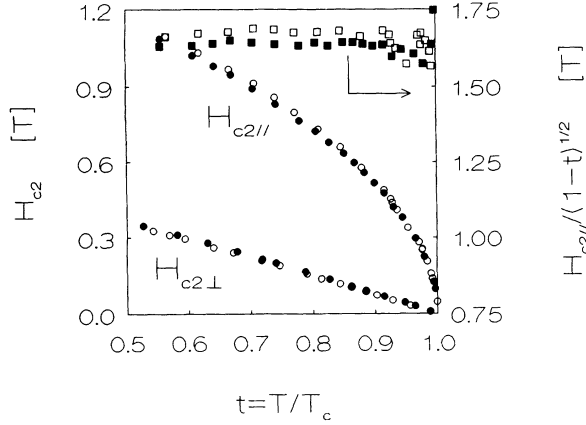


FIG. 6. $H_{c2\parallel}$ and $H_{c2\perp}$ for two samples with different number of layers, 3 nm Fe/ N (40 nm V/1.0 nm Fe)/2 nm Fe with $N=2$ (\circ) and $N=4$ (\bullet) (left-hand axis). In the upper part of the figure, $H_{c2\parallel}/(1-t)^{1/2}$ is displayed for the same samples $N=2$ (\square) and $N=4$ (\blacksquare) (right-hand axis).

side layers, although still smaller than for single thin films. This shows that Eq. (4) cannot be used anymore to determine $\xi(0)$ for a multilayer. In the next section, we will see that also the thickness of d_V influences the slope S . For the monolayer, Eq. (4) is of course valid and gives $\xi(0)=13.9$ nm. This value will also be used for the V in the multilayers.

Concluding this section, in Fig. 6 we show $H_{c2\parallel}$ and $H_{c2\perp}$ for two samples with a different number of blocks, one with two V layers and one with four V layers, all of the same thickness and sandwiched between Fe layers of 1.0 nm thickness. Clearly and as expected, when V layers are decoupled, the behavior for both multilayers is exactly the same.

B. Critical temperatures and fields: Comparison with theory

In the preceding section, we focused on the decoupling of V layers by the Fe layers. In this section we will study the influence of the thickness of the V layers on the superconducting properties of multilayers with decoupled V layers. These systems have been studied theoretically both in Ginzburg-Landau theory¹¹ and in a microscopic approach.⁴ Especially the last is suitable for comparison with our results, since in that paper the results of the model are compared with the experimental data of Ref. 3 on V/Fe multilayers. Reasonable agreement is obtained, but only if one assumes a rather strong dependence of superconducting parameters of the individual V layers upon their thickness, which does not seem justified. Also, the data for the perpendicular critical fields are very scarce. To make a more systematical comparison, we therefore measured T_c and $H_{c2}(T)$, in both perpendicular and parallel orientations for samples with constant Fe thickness and varying V thickness, 5 nm Fe/2(d_V V/3.0 nm Fe)/2 nm Fe, with $d_V=10, 15, 20, 25, 32.5, 40, 55, 70, 85,$ and 100 nm. Since these samples all have Fe as top and bottom layers, all V layers within the multilayer are identical. In Fig. 7 the results for T_c are displayed. T_c

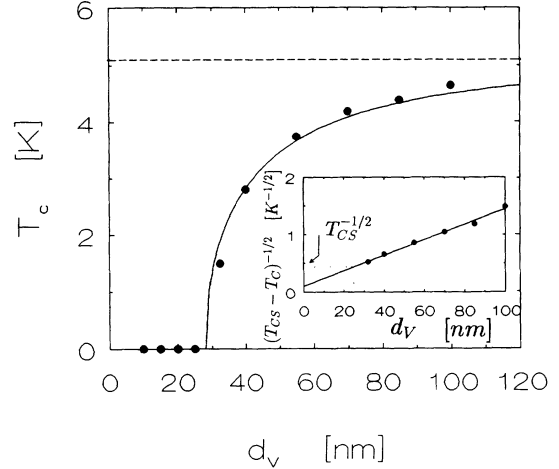


FIG. 7. T_c vs d_V for samples 5 nm Fe/2(d_V V/3.0 nm Fe)/2 nm Fe. Samples with $d_V \leq 25$ nm do not show superconductivity above $T=50$ mK. The line is a fit to the theory as explained in the text, with $\epsilon=5.1$, $T_{CS}=5.1$ K, and $\xi_S=8.8$ nm. The dotted line is T_c for bulk V. The inset shows the phenomenological relation $T_{CS}-T_c \propto d_V^{-2}$.

decreases strongly with decreasing V-layer thickness, as was also found in Refs. 1 and 3. The samples with d_V smaller than 32.5 nm were measured in a dilution refrigerator, but no superconductivity was found for temperatures down to 50 mK. From this we infer the critical V-layer thickness for superconductivity to be approximately 28 nm. Looking at the sample with $d_V=100$ nm, we note that T_c is still lower than for bulk V, even though d_V is much larger than $\xi(0)$ ($=13.9$ nm) for bulk V. Below, we will show that these results are correctly described by the model proposed by Radović *et al.* in Ref. 4.

At this point we want to come back on the T_c oscillations with varying Fe-layer thickness as discussed in the previous section. We have also tried to observe these in multilayers with V inner layers of 25 nm, separated by Fe layers with variable thickness and with 5-nm Fe top and bottom layers. The inner Fe layers ranged between 0.2 and 8 nm. No superconductivity was found for $T > 1.4$ K when $d_{Fe} \geq 0.6$ nm, in accordance with the results above, and also in this set the T_c oscillations (or in this case the reentrance of superconductivity) could not be observed.

Figure 8 shows the $H_{c2\parallel}$ vs T curves for multilayers 5 nm Fe/2(d_V V/3.0 nm Fe)/2 nm Fe, with $d_V=40, 55,$ and 85 nm together with $H_{c2\perp}$ for the 150-nm sputtered monolayer. Close to T_c all multilayers show the 2D behavior as given by Eq. (1). This is indicated by the dashed curves in the figure. For multilayers with $d_V=40$ and 55 nm, this behavior exists in the whole measurable temperature range. The multilayer with $d_V=85$ nm shows a crossover from 2D behavior at temperatures near T_c to 3D behavior of the single V film at low T . Whether this 2D to 3D transition also takes place for the sample with $d_V=55$ nm is difficult to state, since the 3D and 2D behaviors for this sample at low temperatures practically coincide. The 2D to 3D transition is observed for all

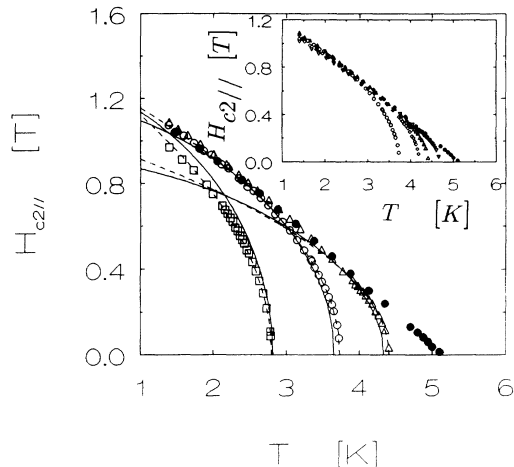


FIG. 8. $H_{c2||}$ for samples with different d_V : 5 nm Fe/ $(d_V$ V/3.0 nm Fe)/2 nm Fe, with $d_V=40$ nm (\square), $d_V=55$ nm (\circ), and $d_V=85$ nm (\triangle). Also shown is H_{c21} for the 150-nm sputtered monolayer (\bullet). Dashed lines indicate the 2D behavior near T_c [Eq. (1)]. Solid lines are predictions of the theory as explained in the text [Eq. (14)] without adjustable parameters. The inset shows the 2D to 3D transition for samples with (going up in T_c) $d_V=55, 70, 85,$ and 100 nm. H_{c21} for the monolayer is also plotted in the inset.

multilayers with $d_V \geq 70$ nm (see the inset of Fig. 8), which means that at low temperatures all V layers with $d_V \geq 70$ nm behave as 3D thick V monolayers. Single V layers in parallel orientation would show a higher critical field than in perpendicular orientation as a result of surface superconductivity, but this (or rather “interface” superconductivity) does not occur in our multilayers, since, at low T , $H_{c2||}$ for the multilayers coincides with H_{c21} of the single V film. We come back to this point below. Note that the 2D to 3D transition in the multilayers is a property of a single V film.

In Fig. 9 we show the H_{c21} vs T curves for the samples

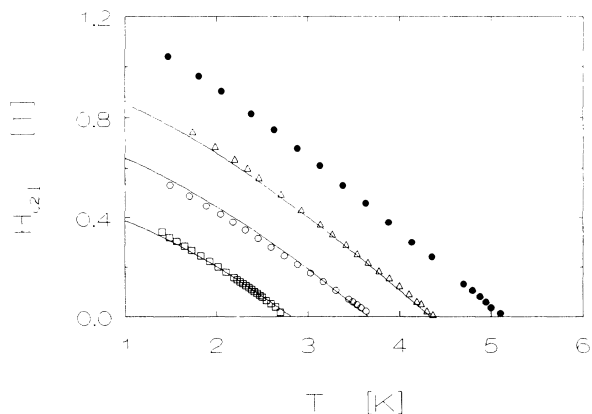


FIG. 9. H_{c21} for the same multilayers as in Fig. 8 and the sputtered monolayer of 150 nm thickness (\bullet). The lines are predictions of the theory as explained in the text [Eq. (16)] without adjustable parameters.

for which $H_{c2||}$ was shown in Fig. 8, together with the result for the sputtered V monolayer. All measurements show linear behavior near T_c , but also the slopes $\partial H_{c21}/\partial T$ differ by less than 15% for all samples in the set and are equal to the slope of the monolayer. The Ginzburg-Landau expression for H_{c21} [Eq. (4)] implies that the slope $\partial H_{c21}/\partial T$ depends upon the product $(\xi(0)^2 T_c)^{-1}$ and thus that the slope should increase with decreasing T_c , assuming that $\xi(0)$ does not depend on the layer thickness d_V . We will see below that the constant slopes are indeed predicted by the model of Ref. 4. Here we only want to note again that for $F/S/F$ multilayers or sandwiches, the GL expression of Eq. (4) clearly cannot be used to deduce $\xi(0)$ from $H_{c21}(T)$.

Next we show that our experimental results are well described by the model put forward in Ref. 4. We will give a brief sketch of the derivation of the basic equations relating the superconducting properties T_c , H_{c21} , and $H_{c2||}$ to the V-layer thickness. The reader is referred to Ref. 4 and references cited therein for the theoretical details. The model is based on the Usadel equations, and it assumes that all S layers are decoupled. The phase transition at H_{c2} is taken to be of second order, so that the Gorkov’s Green’s function describing the condensate of pairs, $F(r, \omega)$ with ω a Matsubara frequency, is described by a linear equation. $F(r, \omega)$ is connected to the pair potential $\Delta = \Delta(r)$ by the self-consistency condition. Using the ansatz that separation of variables can be used and that the space-dependent part of F , $F(r)$, equals $\Delta(r)$, the equations listed below are derived.¹² Since the S layers in the multilayer are decoupled, one only needs to consider one S layer embedded between two F layers to find the multilayer behavior. The coordinate system is chosen so that the interfaces are parallel to the yz plane and the center of the S layer is at $x=0$.

For the superconducting material, one has

$$\Pi^2 F_S = -k_S^2 F_S, \quad (5)$$

where $\Pi = \nabla + 2\pi i A / \phi_0$ is the gauge-invariant gradient with A the vector potential. The eigenvalue $k_S(t)$, with $t = T/T_{cS}$ and T_{cS} the bulk transition temperature for the S material, is related to an effective pair-breaking parameter $\rho(t)$ by

$$k_S^2 = 2\rho / \xi_S^2. \quad (6)$$

Here the S material parameter ξ_S is given by

$$\xi_S = (\hbar D_S / 2\pi k_B T_{cS})^{1/2}, \quad (7)$$

with D_S the diffusion coefficient. The GL coherence length at $T=0$, $\xi(0)$, is related to ξ_S by $\xi_S = 2\xi(0)/\pi$. The pair-breaking parameter $\rho(t)$ is related to t by

$$\ln(t) = \Psi(\frac{1}{2}) - \text{Re}\Psi(\frac{1}{2} + \rho/t), \quad (8)$$

with Ψ the digamma function and Re meaning that the real part should be taken.

In the F layers, the predominant pair-breaking mechanism is assumed to be the strong exchange-field effect which polarizes the spins in the Cooper pairs, leading to

the destruction of superconductivity. Therefore the critical temperature for the F material is taken to be zero, but in a multilayer near the interface F_F is nonzero because of the proximity from the S layers. Assuming that the exchange energy I_0 is much larger than $k_B T_{cS}$, the other characteristic energy involved, and that the pair-breaking effect of any real externally applied magnetic field can always be neglected in comparison with the pair breaking of the exchange field, one has an exponential decay for F_F in the F layers,

$$F_F(x) = C_1 \exp(-k_F |x|), \quad (9)$$

with C_1 an arbitrary constant. The characteristic inverse length k_F is independent of T and is given by

$$k_F = 2(1+i)/\xi_F, \quad (10)$$

with

$$\xi_F = (4\hbar D_F / I_0)^{1/2} \quad (11)$$

and D_F the diffusion coefficient in the F material. Note that the decay length of F in the F layers depends upon I_0 and that k_F is a complex quantity, which stems from the fact that the exchange field can be thought to act only on the spin-dependent part of the electrons.

The solutions for F_F and F_S are subject to the generalized de Gennes–Werthamer boundary condition at the S/F interface,

$$\frac{d}{dx} \ln F_S = \eta \frac{d}{dx} \ln F_F \Big|_{x=\pm d_S/2}, \quad (12)$$

with d_S the thickness of the S layer. The parameter η characterizes the interfaces; e.g., in the dirty limit for specular scattering, η is the ratio of the normal-state conductivities σ_S and σ_F , $\eta = \sigma_F / \sigma_S$. From symmetry, F_S should be symmetrical in $x = 0$.

The above set of equations now suffices to calculate T_c for a multilayer as function of d_S . At T_c ($H=0$), Eq. (5) can be solved exactly, $F_S = C_2 \cos(k_{S0}x)$, with k_{S0} the value of k_S at T_c . Inserting this solution together with (9) in (12) results in

$$\varphi_0 \tan(\varphi_0) = (1+i) \frac{d_S / \xi_S}{\varepsilon}, \quad (13)$$

with $\varphi_0 = k_{S0} d_S / 2$ and $\varepsilon = \xi_F / \eta \xi_S$. For given ε and d_S / ξ_S , this equation can be solved, giving k_{S0} , and with Eq. (6) it yields the effective pair-breaking parameter ρ at T_c . Inserting ρ in Eq. (8) then gives T_c for the multilayer. Note that, since ξ_S , d_S , and T_{cS} are known, ε is the only free parameter left.

To compare T_c for our multilayers with the model, we used the experimental results of the sputtered monolayer, $T_{cS} = 5.1$ K and $\xi_S = 8.8$ nm [= $2\xi(0)/\pi$, with $\xi(0) = 13.9$ nm]. Taking $\varepsilon = 5.1$ yields the solid line in Fig. 7. The agreement between experiment and theory is

seen to be very satisfactory, and the critical thickness for superconductivity, ≈ 28 nm, is nicely reproduced. The predicted T_c vs d_V behavior depends strongly on ε , giving a rather small interval for ε values describing the experiments, $\varepsilon = 5.1 \pm 0.2$. Wong and Ketterson³ calculated T_c for a S layer sandwiched between F layers in GL theory, assuming $|\psi_{GL}|^2 \propto \cos(kx)$ for the GL order parameter $|\psi_{GL}|^2$, which is the same space dependence as for F_S discussed above. Under the assumption that the GL order parameter $|\psi_{GL}|^2$ is zero in the magnetic layers and taking the boundary condition that $|\psi_{GL}|^2 = 0$ at the interfaces, they find that $T_{cS} - T_c \propto 1/d_S^2$. In the inset of Fig. 7, we show that our results are also nicely described by this phenomenological relationship, and the prediction for the critical thickness of 30 nm (see the inset for the construction) is in good agreement with the experimental results.

If the S layers are thin enough to exclude vortices, the critical field parallel to the layers, $H_{c2\parallel}(T)$, can be calculated assuming that the nucleation of superconductivity starts in the middle of the film. Under the condition that $2\pi H_{c2\parallel} d_S^2 / (4\phi_0) < 1$, it was shown in Ref. 4 that the final effect of the presence of the field $H_{c2\parallel}$ on the effective pair-breaking parameter $\rho(t)$ can be approximated by

$$\rho(t) = \rho(t_c) + \frac{g(\varphi_0)}{24} \left[\frac{2\pi H_{c2\parallel}}{\phi_0} \right]^2 d_S^2 \xi_S^2. \quad (14)$$

Here $\rho(t_c)$ is the pair-breaking parameter at T_c . The numerical factor $g(\varphi_0)$ is given by

$$g(\varphi_0) = 1 - \frac{3}{2\varphi_0^2} + \frac{3 + 2\varphi_0 \tan \varphi_0}{\varphi_0^2 + \varphi_0 \tan \varphi_0 + (\varphi_0 \tan \varphi_0)^2}. \quad (15)$$

It should be noted that once ε [and thus $\rho(t_c)$ for given d_S] has been obtained from the fit of T_c vs d_S , Eq. (14) does not contain any free adjustable parameter anymore. For given t , $\rho(t)$ can be calculated with Eq. (8), and equating to Eq. (14) yields $H_{c2\parallel}(t)$. In Fig. 8 we compare our data for $H_{c2\parallel}$ with Eq. (14) using $\varepsilon = 5.1$ as obtained from the T_c vs d_S data. The agreement between data and theory is again very satisfactory in the regime where the multilayers behave as 2D superconductors, since both the T dependence and the magnitude of $H_{c2\parallel}$ are correctly described. Since in Eq. (14) the S layers are assumed to be 2D, the 2D to 3D crossover for $d_V = 85$ nm cannot be reproduced. The model sketched above was recently extended for $F/S/F$ triple layers with S layers of arbitrary thickness.¹³ We will not reproduce those calculations here, but 2D to 3D crossovers are predicted above a certain thickness d_{Ser} of the S layers. This thickness d_{Ser} would be equal to $1.8\xi(T)$ for a thin film in vacuum, but is larger for the $F/S/F$ case and depends on the value of ε . If ε is not too small, it is even possible that $H_{c2\parallel}$ is enhanced over $H_{c2\perp}$ in a manner similar to the nucleation of surface superconductivity. Enhancement would not take place for $\varepsilon = 5.1$, in agreement with the observations that $H_{c2\parallel}$ for multilayers with $d_V \geq 70$ nm coincides with

$H_{c2\perp}$ for the monolayer at low temperatures (see the inset of Fig. 8). Also, $\varepsilon=5.1$ corresponds to $d_{scr}\approx 4\xi_S$, so that below $d_V\approx 35$ nm no crossover can occur down to $T=0$, in good qualitative agreement with the 2D behavior for the multilayer with $d_V=40$ nm in the whole measured temperature range.

For perpendicular fields the expression for the pair-breaking parameter $\rho(t)$ becomes

$$\rho(t)=\rho(t_c)+\frac{\pi H_{c2\perp}}{\phi_0}\xi_S^2. \quad (16)$$

Again, it should be noted that for given ε this expression does not contain any free parameters. In Fig. 9 it is shown that the experimental data are well described by the model. The linear T dependence of $H_{c2\perp}$ close to T_c is well reproduced, as well as the independence on d_V of the slope of $H_{c2\perp}$ for T near T_c .

The results above show that the model proposed by Radović *et al.*⁴ describes all our results satisfactorily. The only fitting parameter ε is found to be 5.1. It is now interesting to see the implications for the characteristic decay length ξ_F of the Green's function F_F in the F material [Eqs. (9)–(11)]. Our results showed that only 0.6-nm Fe layers completely decouple the V layers. Assuming that the V bands are not polarized and that the exponential decay of the F function therefore starts at the physical interfaces, this implies that ξ_F is of the order of 0.6 nm. With $\xi_F=\varepsilon\eta\xi_S=\eta 44.9$ nm, the interface parameter η should be less than 0.013. It is difficult to comment on this value since much is unknown about the interface scattering. The measured values for the specific resistivities at $T=3.5$ K of single films of Fe and V are 6.2 and 6.9 $\mu\Omega$ cm, respectively, with a ratio σ_F/σ_S of the order of 1. On the other hand, these values are mainly determined by grain-boundary scattering in the plane of the film, which is not relevant for η . For single-crystalline material, the resistances are much lower, 0.05 $\mu\Omega$ cm for Fe and 2.5 $\mu\Omega$ cm for V and the ratio σ_F/σ_S is increased to 50. Most probably, η is for a large part determined by the change of band structure at the interface and not easily accessible by experiment, although resistance measurements perpendicular to the layers might give more information on this. Moreover, since a part of the conduction electrons in Fe is believed to consist of highly polarized itinerant d -like electrons,¹⁴ the scattering may be strongly spin dependent. The low value for η may therefore well be caused by different spin channels, rather than by interface roughness or by different overall conductivity.

The other important parameter entering the model is the exchange energy I_0 . Estimating I_0 from the fitting procedure above again requires rough assumptions. Again, taking $\xi_F=0.6$ nm, we can try to make an estimation for $I_0=4\hbar D_F/\xi_F^2$. The diffusion coefficient $D_F=lv_F/3$, with l the mean free path and v_F the Fermi velocity, for our thin Fe layers is not exactly known. Even if we take the smallest possible value for l , namely,

the layer thickness of 0.6 nm, and using the typical Fermi velocity for Fe, $v_{Fe}=2\times 10^6$ m/s, this yields $I_0=4.6\times 10^{-19}J\approx 3.0$ eV. Note that if l is taken to be larger than 0.6 nm, I_0 would even increase. The value for I_0 would not be unreasonable if it could be compared to half the exchange splitting of the itinerant d electrons, estimated at about 1 eV,¹⁵ instead of to the s - d exchange energy which is typically a few tenths of an eV. Also, the strong spin-dependent scattering at the nonmagnetic interface would naturally lead to the assumed restriction of the mean free path by the layer thickness.

All parameter values estimated above indicate an important role of the Fe itinerant d electrons. However, since both η would increase and I_0 decrease with increasing ξ_F , we should closely scrutinize the estimate for ξ_F which was obtained by neglecting the possible polarization of electrons in the V layers due to the Fe layers. If polarization were present, the result would be that the exponential decrease of superconductivity would already start deep inside the V layers, instead of starting at the physical Fe/V interface as assumed above. The effective separation between superconducting V material would be larger than just the Fe layer thickness, and a (much) larger decay length for superconductivity than 0.6 nm would follow. Trying to incorporate this idea in the model, we tried to describe the experiments assuming a roughly estimated thickness of 4 nm polarized V on each interface, so that the effective V-layer thickness $d_{V\text{ eff}}$ is 8 nm less than the nominal sputtered thickness. From fitting T_c vs $d_{V\text{ eff}}$, we then obtain $\varepsilon=7$, and both T_c vs $d_{V\text{ eff}}$ and $H_{c2\perp}(T)$ curves are well described by the model. The predicted $H_{c2\parallel}$ values are, however, too high, about 25% for the thinnest sample with $d_V=40$ nm, and so within the assumptions of the model, this picture is not capable of describing all the data consistently.

Finally, we would like to remark here that even though all the data on our V/Fe multilayers can be described with the model of Radović *et al.*, we performed the same type of measurements on V/F multilayers with for F different types of thick ferromagnetic layers, especially Ni and Co, which will be the subject of a separate paper. For all these multilayers, T_c with varying d_V can be accurately fitted, but the critical field data are not as well described as in the V/Fe case.

IV. CONCLUSION

To summarize, we have shown that for well-defined V/Fe multilayers the superconductivity in adjacent V layers is decoupled by only 0.6-nm-thick Fe layers. This is concluded from the independence of the superconducting properties T_c , $H_{c2\parallel}$, and $H_{c2\perp}$ on $d_{Fe}\geq 0.6$ nm, as well as from the 2D temperature dependence of $H_{c2\parallel}$ for thick multilayers with thin V layers. A “ π -contact” superconducting ground state does not exist in our multilayers, in contrast with suggestive results on V/Fe multilayers by Wong *et al.*³ We have also shown that T_c and both $H_{c2\parallel}$ and $H_{c2\perp}$ can be consistently and very nicely described by

the model of Radović *et al.*, using only one adjustable parameter. The manner in which the effect of magnetism is introduced in the problem appears to be a correct approach. The values found for the interface characterization parameter η and the exchange energy I_0 indicate that the itinerant d electrons of Fe play an important role in the destruction of the Cooper pairs. A better microscopic understanding especially of the spin dependence of the scattering at the interfaces is still needed.

ACKNOWLEDGMENTS

The authors would like to thank Dr. A. E. Koshelev, Professor J. A. Mydosh, and Professor P. H. Kes for stimulating discussions. E. van de Laar is kindly acknowledged for performing the measurements in the dilution refrigerator. This work was sponsored in part by the Netherlands Foundation for the Fundamental Research on Matter (FOM).

¹J. J. Hauser, H. C. Theuerer, and N. R. Werthamer, *Phys. Rev.* **142**, 118 (1966).

²H. K. Wong and J. B. Ketterson, *J. Low Temp. Phys.* **63**, 139 (1986).

³H. K. Wong, B. Y. Jin, H. Q. Yang, J. B. Ketterson, and J. E. Hilliard, *J. Low Temp. Phys.* **63**, 307 (1986).

⁴Z. Radović, L. Dobrosavljević-Grujić, A. I. Buzdin, and J. R. Clem, *Phys. Rev. B* **38**, 2388 (1988).

⁵Z. Radović, M. Ledvij, L. Dobrosavljević-Grujić, A. I. Buzdin, and J. R. Clem, *Phys. Rev. B* **44**, 759 (1991).

⁶A. I. Buzdin, M. Yu. Kupriyanov, and B. Vujičić, *Physica C* **185-189**, 2025 (1991).

⁷L. N. Bulaevskii, V. V. Kuzii, and A. A. Sobyenin, *Pis'ma Zh. Eksp. Teor. Fiz.* **25**, 314 (1977) [*JETP Lett.* **25**, 290 (1977)].

⁸M. V. Nevitt and A. T. Aldred, *J. Appl. Phys.* **34**, 463 (1963).

⁹I. O. Kulik, *Solid State Commun.* **19**, 535 (1976).

¹⁰C. G. Granqvist and T. Claeson, *Solid State Commun.* **32**, 531 (1979).

¹¹H. Schinz and F. Schwabl, *J. Low Temp. Phys.* **88**, 347 (1992).

¹²This ansatz yields an approximate solution for the Usadel equations and amounts to a generalization of the de Gennes–Werthamer approach. An exact solution could lead to qualitative different results, especially when the S layers in the multilayer are not completely decoupled, but for decoupled, not too thin S layers sandwiched between strong ferromagnetic material, the two approaches lead to qualitatively the same results. See Ref. 5 and Z. Radović, M. L. Ledvij, and L. Dobrosavljević-Grujić, *Solid State Commun.* **80**, 43 (1991).

¹³M. Ledvij, L. Dobrosavljević-Grujić, Z. Radović, and J. R. Clem, *Phys. Rev. B* **44**, 859 (1991).

¹⁴M. B. Stearns, *J. Magn. Mater.* **104-107**, 1745 (1992).

¹⁵For this estimate we use $k_F^\uparrow = 11 \text{ nm}^{-1}$, $k_F^\downarrow = 4 \text{ nm}^{-1}$ from Ref. 14 and an effective mass $m^* = 2$; see M. B. Stearns, *Phys. Rev. B* **8**, 4383 (1973). The full exchange splitting from these numbers is 2 eV. In Ref. 4, the full splitting is implicitly defined as $2I_0$, so our I_0 is half the splitting.